Enhanced Bearing Fault Diagnosis Using Statistical Time Features and Independent Component Analysis: A Comparative Study of Neural and Non-Neural Models

Abstract. Bearing fault diagnosis is essential for the efficient maintenance of rotating machinery, but it presents challenges due to the complexity and non-stationary nature of vibration signals. This study aims to enhance the accuracy of bearing fault diagnosis by identifying key Statistical Time Features (STFs) from vibration signals to classify normal bearings and three fault types: inner race, outer race, and roller faults. Independent Component Analysis (ICA) was used for dimensionality reduction. A comparative analysis was conducted between neural and non-neural classifiers, where models were initially trained on nine STFs, followed by a reduced set of five STFs obtained through ICA. Both neural networks (NN) and non-neural models achieved higher accuracy using the reduced set of STFs compared to the full set. Among the classifiers, the Narrow Neural Network emerged as the best-performing neural model, while the Random Forest and Ensemble Bagged Tree showed superior performance among non-neural classifiers. These results underscore the value of feature selection and dimensionality reduction in enhancing the precision and accuracy of bearing fault diagnosis.

Keywords: bearing, fault Diagnosis, statistical time features, independent component analysis, neural classifiers, non-neural classifiers

1 Introduction

Bearings play an important role in rotating machinery, ensuring the smooth functioning of various engineering systems, such as electric motors used in industries like power generation, manufacturing, and transportation. Despite their robustness, bearings account for over 51% of induction motor failures [1]. These failures can result in costly downtime, making early detection essential for condition-based maintenance (CBM). Common causes of bearing failure include improper installation, lubrication problems, and mechanical damage, which can lead to catastrophic system failures.

Recent research has focused on improving maintenance solutions for these machines, particularly through the application of machine learning (ML) techniques [2]. Non-destructive monitoring methods, including vibration and acoustic analysis, have become widely adopted for detecting bearing faults [3]. Studies have made notable advancements in identifying rolling bearing defects and analyzing their characteristics through various techniques [4].

One of the main challenges in fault diagnosis (FD) is developing intelligent systems that can autonomously detect and classify bearing conditions. Feature extraction has been extensively used in FD, utilizing time, frequency, and time-frequency domain analyses to identify key fault characteristics. Advanced techniques like ML, deep

learning (DL), and statistical models such as autoencoders, generative adversarial networks (GANs), and SVMs have significantly improved detection accuracy [5]. Studies have also shown the potential of wavelet energy in identifying system failures, especially in vibration signals, which often exhibit nonlinear and non-stationary behavior [6].

Traditional FD methods largely rely on signals like vibration acceleration, stator current, and acoustic emission (AE) [7]. While vibration-based approaches work better at high speeds, AE-based methods are more effective at detecting early-stage defects at lower speeds by capturing low-energy acoustic emissions from developing cracks [8]. However, diagnosing faults under varying operating conditions remains challenging, as many methods depend on speed-specific characteristic defect frequencies (CDFs), which may become inconsistent when speed fluctuates.

Wavelet transforms, which enhance the localized properties of the short-time Fourier transform (STFT), are highly effective for time-frequency analysis due to their flexible windowing based on frequency [9]. However, they require predefined wavelet basis functions, and the choice of these functions heavily influences the results, limiting adaptability. On the other hand, empirical mode decomposition (EMD) decomposes signals based on time-domain characteristics without predefined functions, offering greater flexibility [10]. Despite its advantages, EMD is susceptible to challenges such as modal distortion and endpoint effects, which diminish its effectiveness. To overcome these issues, methods like ensemble EMD and improved EMD have been developed, though they remain computationally demanding and less effective for diagnosing bearing signals with discontinuous phases [11].

Feature preprocessing is an important step in the fault diagnosis process, as it involves evaluating and selecting discriminant features from the extracted fault indicators. The quality of these features directly influences the classifier's generalization and classification performance [12]. Past approaches like probabilistic principal component analysis (PCA), trace ratio LDA, and sensitive discriminant analysis have been used to create discriminant feature spaces. However, PCA-based methods often struggle with class separation and information loss, while LDA’s effectiveness can be impacted by the penalty graph representation of features from different classes [13].

To address these limitations, this paper proposes a methodology focused on feature extraction from real-world accelerometer data collected from bearings operating under normal and various cracked conditions. The primary goal is to identify distinct fault patterns for classification analysis. Specifically, nine statistical time-domain features (STFs) will be extracted from the accelerometer data to capture critical information about the bearing’s operational state. To enhance classification performance, ICA will be combined with Recursive Feature Elimination (RFE), utilizing a Random Forest algorithm, to reduce the dimensionality of the feature set. This refined feature set will then be used to train classification models. A comparative analysis will be conducted between classifiers trained on the original nine STFs and those trained on the optimized five-feature set to evaluate improvements in fault detection performance and overall classification accuracy.

1. The study proposes a dual-feature extraction strategy by utilizing both STFs and ICA for dimensionality reduction, improving bearing fault diagnosis accuracy in rotating machinery.
2. The study enhances the interpretability of bearing fault diagnosis by applying RFE, ensuring that the most relevant features are retained while minimizing computational complexity.
3. The proposed methods are evaluated using real-world vibration signal data from bearings under normal and faulty conditions.

2 Proposed methodology

The approach taken in this study is described as follows: Figure 1 shows the graphical flow of the proposed methodology.

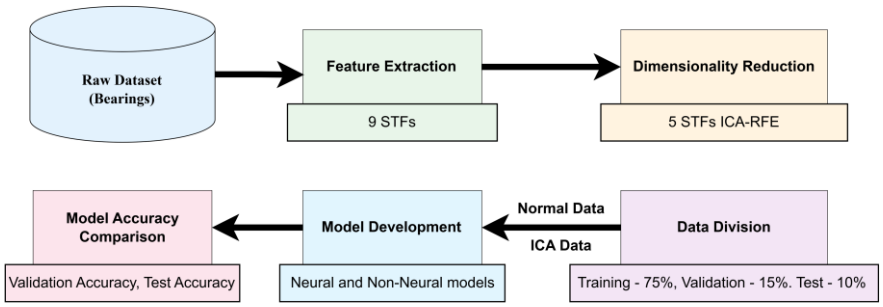

Figure 1. Flow diagram of the proposed method

Step 1: The dataset comprised vibration signals collected from bearings under four conditions: inner race fault (IRF), outer race fault (ORF), roller defects, and normal operation, representing distinct classes for multi-class classification. The time-series data were pre-processed for uniformity and imported into a Python environment for analysis.
Step 2: Feature engineering was applied to enhance classification. The raw signals were transformed into nine features, including mean, standard deviation, kurtosis, and skewness, which captured important statistical characteristics of the vibration data, highlighting patterns related to bearing health or failure.
Step 3: Exploratory data analysis was conducted to understand feature distributions and correlations. t-SNE visualized feature separability in 2D, while ICA and RFE reduced the feature set to five key attributes. RFE helped select the top-ranking features for further model training, minimizing complexity.
Step 4: The dataset was normalized using min-max scaling and split into training, validation, and test sets. Various models, including decision trees, Naive Bayes, SVMs, Random Forests, and neural networks, were trained. Hyperparameters were optimized through cross-validation.

Step 5: Models were trained using both the original nine features and the reduced five features from ICA and RFE. Performance was evaluated using validation accuracy, test accuracy, and confusion matrices. Top-performing models, including Random Forest, Ensemble Bagged Tree, and Narrow NN, achieved high accuracy.

3 Technical Background

3.1 Feature Engineering

In this research, nine STFs were engineered to extract meaningful insights from the raw vibrational data recorded during bearing operations under different conditions. The transformation of raw time-series vibration signals into a structured set of statistical features was useful to ensure that the models could effectively learn the fault patterns. The nine STFs extracted are listed in Table 1, where each feature contributes distinct information about the vibration behavior of the bearings. These features, ranging from basic descriptive statistic domain characteristics, extract key patterns of bearing health. For example, mean (F1) provides a central measure of the signal, while kurtosis (F5) and skewness (F6) offer insights into the distribution and symmetry of the vibration data. Similarly, features like RMS (F4) and crest factor (F9) are important for identifying the severity and impact of bearing faults. The integration of these STFs played an important role in distinguishing between normal and faulty conditions. As the bearing faults progressed over time, the statistical patterns captured by these features became more pronounced, particularly in the later stages of degradation.

Table 1. Nine Statistical Time Features

STF	Description
F1	Mean
F2	Maximum Value
F3	Minimum Value
F4	Root Mean Square (RMS)
F5	Kurtosis
F6	Skewness
F7	Standard Deviation
F8	Form Factor
F9	Crest Factor

3.2 Dimensionality Reduction - ICA-RFE

Dimensionality reduction is the main step in preparing data for ML models, as it reduces the complexity of the dataset while preserving the most significant information. In this study, ICA was employed to reduce the nine extracted STFs to a smaller set of uncorrelated features, allowing for faster training and improved generalization of the models. The Pareto chart in Figure 2 (a) demonstrates the cumulative variance explained by the principal components. It shows that the first five components capture

over 98% of the total variability in the dataset. This finding confirmed that the dimensionality of the feature space could be safely reduced from nine to five components without significant loss of information. The first two components, IC1 and IC2, were particularly important, attaining most of the variance and contributing to the most significant separation between the classes.

In addition to variance analysis, ICA was used to visualize the data in lower dimensions. Figure 2 (b) presents a 2D scatter plot of the data points projected onto the first two components, revealing clusters of data corresponding to the different fault types. This visualization confirmed that the ICA-transformed features retained meaningful separation between classes, with distinct clusters for IRF, ORF, roller faults, and normal operation. This dimensionality reduction was essential for ensuring that the models could be trained efficiently while maintaining high accuracy. The reduced feature set of five components not only sped up the training process but also helped avoid the risk of overfitting that can arise when using a high-dimensional feature space.

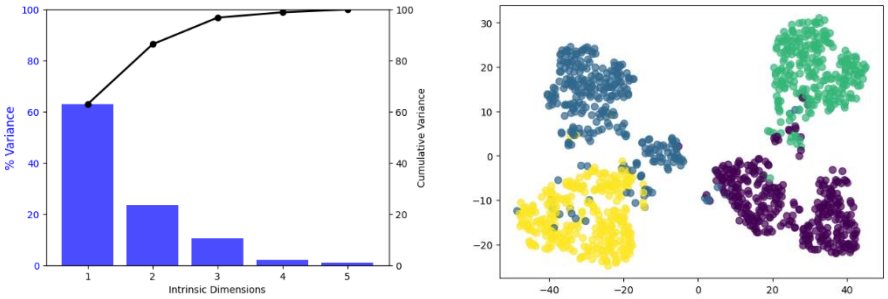

Figure 2. (a) Variance explained by components using Pareto Chart **(b)** 2D t-SNE visualization of the feature set

4 Results and Performance Evaluation

The evaluation of fault diagnosis in this study was conducted across the dataset used for classification, which consists of four distinct bearing conditions. To ensure a fair and consistent evaluation process, the dataset was split into training, validation, and testing sets with a 75%-15%-10% ratio, where 75% of the data was reserved for model training, 15% for validation and the remaining 10% for testing. Additionally, a 10-fold cross-validation strategy was employed to validate the models' performance. In this strategy, the dataset was randomly shuffled and partitioned into 10 subsets. For each iteration, one subset was selected as the validation set, while the remaining nine subsets were used for training the model. This cross-validation was repeated 10 times, ensuring that every sample was used in the validation set exactly once, which helped mitigate the effects of overfitting and provided a more robust evaluation of the models.

4.1 Experimental setup

This experiment investigated the behavior of **KBC30206J** roller bearings under both normal and defective conditions, including outer race fault, roller defects, and inner race fault. The experimental setup and its schematics are presented in Figure 3. The bearing was operated at a constant speed of 1800 RPM under an axial load of 100 kg, with radial and axial loads applied to simulate real-world conditions. Vibration data were captured using two PCB-622B01 accelerometers positioned vertically and horizontally on the bearing housing, with a frequency range of 0.2 to 15,000 Hz, a measurement range of ±490 m/s², and a sensitivity of 100 mV/g. Data acquisition was managed using a National Instruments NI 9234 DAQ system, offering 24-bit resolution and a dynamic range of 102 dB. Baseline data from healthy bearings were recorded over 5-minute intervals in comparison with data collected after introducing artificial defects. Faults in the outer race, roller, and inner race measured approximately 3 mm by 1.5 mm by 1 mm. Vibration data were analyzed to identify characteristic signatures of different defects and develop diagnostic models for bearing fault detection. The details of the data collected during the experiment are described below in Table 2.

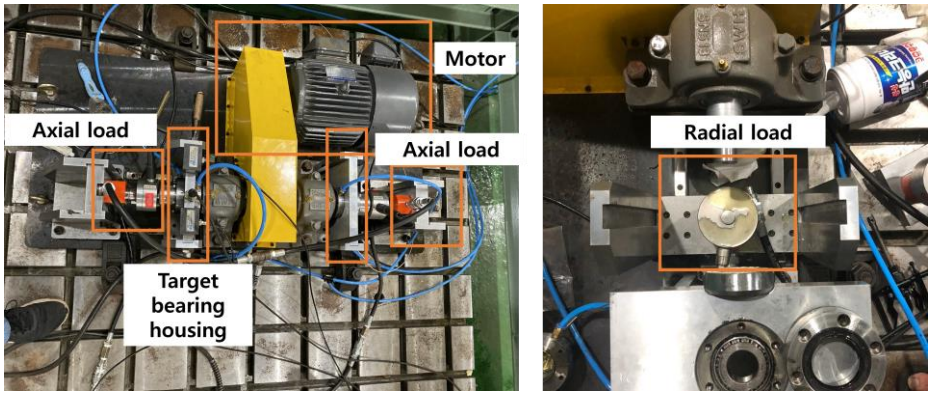

Figure 3. Experimental Setup

Table 2. Summary of the utilized Dataset

Bearing Condition	Data Samples	Sampling Frequency	Recording Time
Normal	300	15K Hz	300 seconds
Inner Race Fault	300	15K Hz	300 seconds
Outer Race Fault	300	15K Hz	300 seconds
Roller Fault	300	15K Hz	300 seconds

4.2 Performance evaluation and comparison

To measure the effectiveness of the classification models, several key performance metrics were used, including recall, precision, F1-score, and overall classification accuracy through equation (1) to equation (4). These metrics were chosen to provide a balanced evaluation across all fault categories, ensuring that the model's performance is not skewed by class imbalances. Through this comprehensive evaluation process, the models' performance was assessed not only on their ability to accurately classify the different bearing fault types but also on their generalization capabilities across varying subsets of data. This ensures that the final selected models are reliable and well-suited for practical applications in bearing fault diagnosis and predictive maintenance.

$$Accuracy = \frac{(TN + TP)}{(TP + TN + FP + FN)} \times 100\% \quad (1)$$

$$Precision = \frac{TP}{TP + FP} \times 100\% \quad (2)$$

$$Recall = \frac{TP}{TP + FN} \times 100\% \quad (3)$$

$$F1 - Score = \frac{2TP}{2TP + FP + FN} = \frac{2 \times (Precision \times Recall)}{Precision + Recall} \quad (4)$$

This study utilizes real-time bearing data from different classes. Initially, both neural and non-neural classification models were trained using all nine STFs. However, some features were redundant and did not significantly contribute to model performance, reducing accuracy and effectiveness. Feature reduction techniques were applied, specifically IDA with RFE using an RF algorithm, refining the feature set to the five most relevant ones for effective pattern recognition.

Our experiments revealed that, on average, models achieved accuracy levels above 90%. The results, as presented in Table 3, demonstrate that the optimized feature set significantly improved model accuracy and efficiency. Models trained with the reduced five STFs outperformed those trained with the full nine-feature set. Neural models, known for learning complex patterns, demonstrated strong resilience to feature reduction. Even with fewer features, these models maintained high classification accuracy, confirming that eliminating redundant features did not impact performance.

For model evaluation, the confusion matrix and t-SNE were analyzed to determine the best classifiers. Among non-neural models, the Random Forest and Ensemble Bagged Tree showed high robustness across all class labels. In neural models, the Narrow NN performed exceptionally well, indicating superior classification capability. This was further confirmed through the evaluation of the confusion matrix and t-SNE plots, as shown in Figures 4 and 5.

Table 3. Classification Models Results.

Classifier	9 Features		5 ICA Features	
	Validation Accuracy	**Test Accuracy**	**Validation Accuracy**	**Test Accuracy**
Random Forest	94.4	93.43	96.59	98.54
Fine Tree	94.15	96.6	96.1	97.57
Medium Tree	94.63	96.12	93.17	94.17
Linear Discriminant	92.2	93.69	94.15	94.66
Quadratic Discriminant	92.2	96.6	96.59	96.6
Linear SVM	97.07	99.03	96.59	97.57
Quadratic SVM	87.32	92.72	81.95	80.58
Cubic SVM	93.66	97.57	94.15	96.6
Fine Gaussian SVM	97.07	99.51	96.59	97.57
Medium Gaussian SVM	97.07	97.11	96.1	98.54
Coarse Gaussian SVM	98.05	97.06	97.07	96.6
Fine KNN	97.56	98.06	93.66	96.12
Medium KNN	97.07	97.57	96.1	98.06
Weighted KNN	96.59	97.57	96.1	97.57
Ensemble Bagged Tree	93.43	94.89	97.56	98.54
Ensemble Subspace KNN	88.81	89.54	90.73	91.75
Narrow NN	96.59	99.03	96.1	98.06
Medium NN	98.05	100	97.07	97.57
Wide NN	98.54	99.51	96.59	97.09
Bilayered NN	98.54	99.51	96.59	97.57
Trilayered NN	97.56	97.57	96.59	97.09

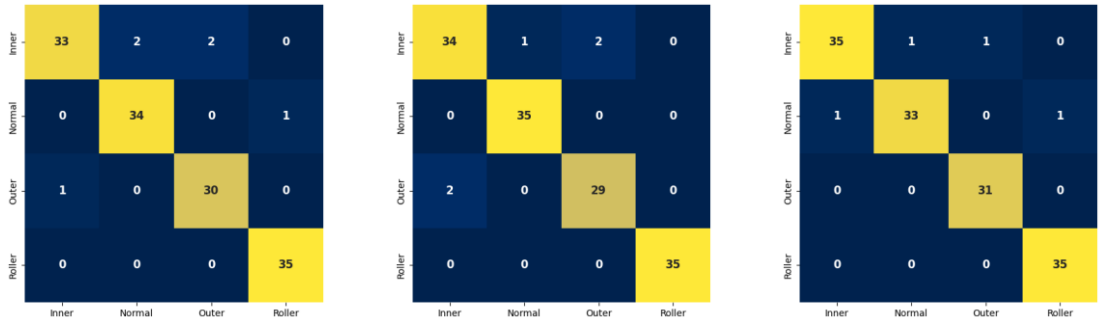

(a) (b) (c)

Figure 4. Confusion Matrix of **(a)** Random Forest **(b)** Ensemble Bagged Tree **(c)** Narrow NN

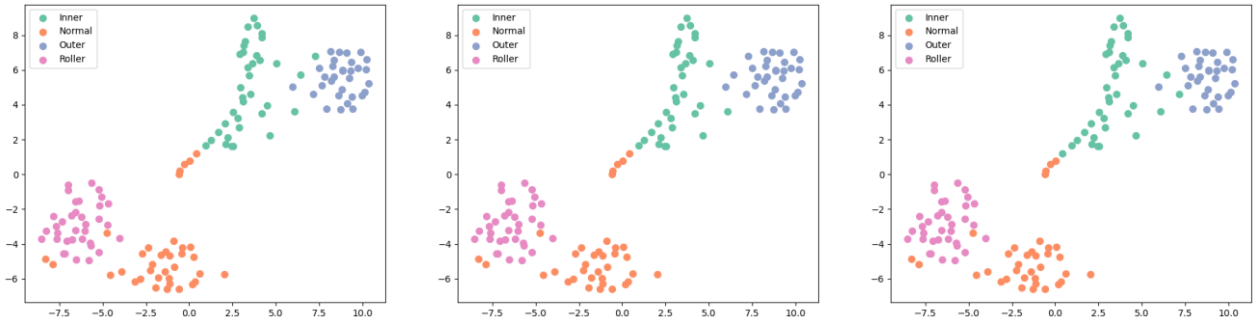

(a) (b) (c)

Figure 5. t-SNE of **(a)** Random Forest **(b)** Ensemble Bagged Tree **(c)** Narrow NN

This streamlined approach simplified the classification process and enhanced overall model effectiveness. Both neural and non-neural models achieved superior outcomes using the optimized feature set compared to the full set. These findings highlight the importance of feature selection in classification, as removing less informative features improved the models' ability to detect patterns and make accurate classifications. Ultimately, the combination of ICA and RFE optimized feature selection, leading to more efficient and accurate performance across both neural and non-neural models.

5 Conclusion

This research focused on classifying bearing conditions normal, IRF, ORF, and roller element fault using STFs. A comprehensive comparison was made between neural and non-neural classifiers, utilizing two feature sets: the original set of nine STFs and a reduced set of five STFs. The results showed that the reduced ICA-RFE feature set consistently provided more accurate classification across all models compared to the full STF set. Among the classifiers, the RF, Ensemble Bagged Tree, and Narrow NN models performed best, achieving high classification accuracy with both the full and reduced feature sets. Future work will explore advanced deep learning techniques, such as convolutional neural networks and recurrent neural networks, to further enhance classification accuracy and improve fault detection.

References

[1] A. S. Maliuk, A. E. Prosvirin, Z. Ahmad, C. H. Kim, and J.-M. Kim, “Novel Bearing Fault Diagnosis Using Gaussian Mixture Model-Based Fault Band Selection,” *Sensors*, vol. 21, no. 19, p. 6579, Oct. 2021, doi: 10.3390/s21196579.

[2] A. S. Maliuk, Z. Ahmad, and J.-M. Kim, “Hybrid Feature Selection Framework for Bearing Fault Diagnosis Based on Wrapper-WPT,” *Machines*, vol. 10, no. 12, p. 1204, Dec. 2022, doi: 10.3390/machines10121204.

[3] M. He and D. He, “Deep Learning Based Approach for Bearing Fault Diagnosis,” *IEEE Trans Ind Appl*, vol. 53, no. 3, pp. 3057–3065, May 2017, doi: 10.1109/TIA.2017.2661250.

[4] Y. Gao, Z. Ahmad, and J.-M. Kim, “Fault Diagnosis of Rotating Machinery Using an Optimal Blind Deconvolution Method and Hybrid Invertible Neural Network,” *Sensors*, vol. 24, no. 1, p. 256, Jan. 2024, doi: 10.3390/s24010256.

[5] S. Zhang, S. Zhang, B. Wang, and T. G. Habetler, “Deep Learning Algorithms for Bearing Fault Diagnostics—A Comprehensive Review,” *IEEE Access*, vol. 8, pp. 29857–29881, 2020, doi: 10.1109/ACCESS.2020.2972859.

[6] D.-T. Hoang and H.-J. Kang, “A survey on Deep Learning based bearing fault diagnosis,” *Neurocomputing*, vol. 335, pp. 327–335, Mar. 2019, doi: 10.1016/j.neucom.2018.06.078.

[7] S. A. McInerny and Y. Dai, “Basic vibration signal processing for bearing fault detection,” *IEEE Transactions on Education*, vol. 46, no. 1, pp. 149–156, Feb. 2003, doi: 10.1109/TE.2002.808234.

[8] Z. Ahmad, M. F. Siddique, N. Ullah, J. Kim, and J.-M. Kim, “Centrifugal Pump Health Condition Identification Based on Novel Multi-filter Processed Scalograms and CNN,” 2024, pp. 162–170. doi: 10.1007/978-3-031-53830-8_16.

[9] D. HO and R. B. RANDALL, “OPTIMISATION OF BEARING DIAGNOSTIC TECHNIQUES USING SIMULATED AND ACTUAL BEARING FAULT SIGNALS,” *Mech Syst Signal Process*, vol. 14, no. 5, pp. 763–788, Sep. 2000, doi: 10.1006/mssp.2000.1304.

[10] N. Ullah, M. F. Siddique, and J.-M. Kim, “A Hybrid Classification Framework of Centrifugal Pumps Using Wavelet Coherence Visuals and Principal Component Analysis,” in *2023 IEEE International Conference on High Performance Computing & Communications, Data Science & Systems, Smart City & Dependability in Sensor, Cloud & Big Data Systems & Application (HPCC/DSS/SmartCity/DependSys)*, IEEE, Dec. 2023, pp. 906–911. doi: 10.1109/HPCC-DSS-SmartCity-DependSys60770.2023.00131.

[11] S. Ullah, Z. Ahmad, and J.-M. Kim, “Fault Diagnosis of a Multistage Centrifugal Pump Using Explanatory Ratio Linear Discriminant Analysis,” *Sensors*, vol. 24, no. 6, p. 1830, Mar. 2024, doi: 10.3390/s24061830.

[12] B. Li, M.-Y. Chow, Y. Tipsuwan, and J. C. Hung, “Neural-network-based motor rolling bearing fault diagnosis,” *IEEE Transactions on Industrial Electronics*, vol. 47, no. 5, pp. 1060–1069, 2000, doi: 10.1109/41.873214.

[13] H. Li, T. Liu, X. Wu, and Q. Chen, “An optimized VMD method and its applications in bearing fault diagnosis,” *Measurement*, vol. 166, p. 108185, Dec. 2020, doi: 10.1016/j.measurement.2020.108185.